Nano Energy 56 (2019) 693–699

Contents lists available at ScienceDirect

Nano Energy

journal homepage: www.elsevier.com/locate/nanoen

Full paper

Solution-synthesized chiral piezoelectric selenium nanowires for wearable self-powered human-integrated monitoring

Min Wu[a,b], Yixiu Wang[a,b], Shengjie Gao[a,b], Ruoxing Wang[a,b], Chenxiang Ma[a,b,c], Zhiyuan Tang[c], Ning Bao[d,e], Wenxuan Wu[f,*], Fengru Fan[g,*], Wenzhuo Wu[a,b,h,i,**]

[a] School of Industrial Engineering, Purdue University, West Lafayette, IN 47907, USA
[b] Flex Laboratory, Purdue University, West Lafayette, IN 47907, USA
[c] Department of Applied Chemistry, School of Chemical Engineering and Technology, Tianjin University, Tianjin 300072, China
[d] School of Public Health, Nantong University, Nantong, Jiangsu, 226019, China
[e] Key Laboratory of Sensor Analysis of Tumor Marker, Ministry of Education, College of Chemistry and Molecular Engineering, Qingdao University of Science and Technology, Qingdao, Shandong, 266042, China
[f] Shenzhen Broadthink Advanced Materials Technologies Co., Ltd., Shenzhen, Guangdong 518117, China
[g] Department of Chemistry & Biochemistry, University of California, Santa Barbara, CA 93106, USA
[h] Birck Nanotechnology Center, Purdue University, West Lafayette, IN 47907, USA
[i] Regenstrief Center for Healthcare Engineering, Purdue University, West Lafayette, IN 47907, USA

ARTICLE INFO

Keywords:
Piezoelectric device
Selenium nanowires
Self-powered sensor
Wearable electronics
Human physiological monitoring

ABSTRACT

Smart sensing devices with high stretchability and self-powered characteristics are essential in future generation wearable human-integrated applications. Here we report for the first time scalable synthesis and integration of selenium (Se) nanowires into wearable piezoelectric devices, and explore the feasibility of such devices for self-powered sensing applications, e.g., physiological monitoring. The ultrathin device can be conformably worn onto the human body, effectively converting the imperceptible time-variant mechanical vibration from the human body into distinguishable electrical signals, e.g., gesture, vocal movement, and radial artery pulse, through straining the piezoelectric Se nanowires. Our results suggest the potential of solution-synthesized Se nanowire a new class of piezoelectric nanomaterial for self-powered biomedical devices and opens doors to new technologies in energy, electronics, and sensor applications.

1. Introduction

In 2006, Wang *et al.* invented ZnO-based piezoelectric nanogenerators (PENG) which could realize the conversion of mechanical energy from the ambient environment into electrical power [1]. Since then, the harvesting of mechanical energy using nanostructured piezoelectric materials has received considerable attention, including wurtzite materials like GaN [2–4], CdS [5,6], perovskite materials like $BaTiO_3$ [7–10], $ZnSnO_3$ [11–13], other inorganic lead-free piezoelectric material [14,15] and also synthetic polymers such as PVDF and its copolymers [16–18]. The low-dimensional geometries, superior mechanical properties of piezoelectric nanomaterials compared to their bulk counterparts, and the direct energy conversion in piezoelectric process facilitate the integration into deformable devices for efficiently harvesting ubiquitous mechanical energy, hinged on principles of the time-variant piezoelectric polarization induced displacement current [19]. Ongoing efforts in the field of PENG are primarily focused on improving energy conversion by further enhancing the materials' piezoelectric properties [16,20–22] and demonstrating proof-of-concept application [23]. Progress in these fields combined with the emerging methods for deterministic production and assembly of nanomaterials [21] leads to exciting research opportunities. Nevertheless, significant roadblocks exist for realizing the technological potential of existing piezoelectric nanomaterials. For instance, the sophisticated process for synthesizing wurtzite-structured piezoelectric nanowires with orientation control limit the potential device integration and applications [24–26]. Obstacles concerning scalable, economic production of piezoelectric nanomaterials with desired piezoelectric and mechanical properties continue to prevail.

Here we demonstrate for the first time scalable synthesis and integration of selenium (Se) nanowires into wearable piezoelectric devices and explore the feasibility of such devices for self-powered sensing

* Corresponding authors.
** Corresponding author at: School of Industrial Engineering, Purdue University, West Lafayette, IN 47907, USA.
E-mail addresses: wxwu@mail.ustc.edu.cn (W. Wu), fengrufan@ucsb.edu (F. Fan), wenzhuowu@purdue.edu (W. Wu).

https://doi.org/10.1016/j.nanoen.2018.12.003
Received 1 October 2018; Received in revised form 19 November 2018; Accepted 3 December 2018
Available online 06 December 2018

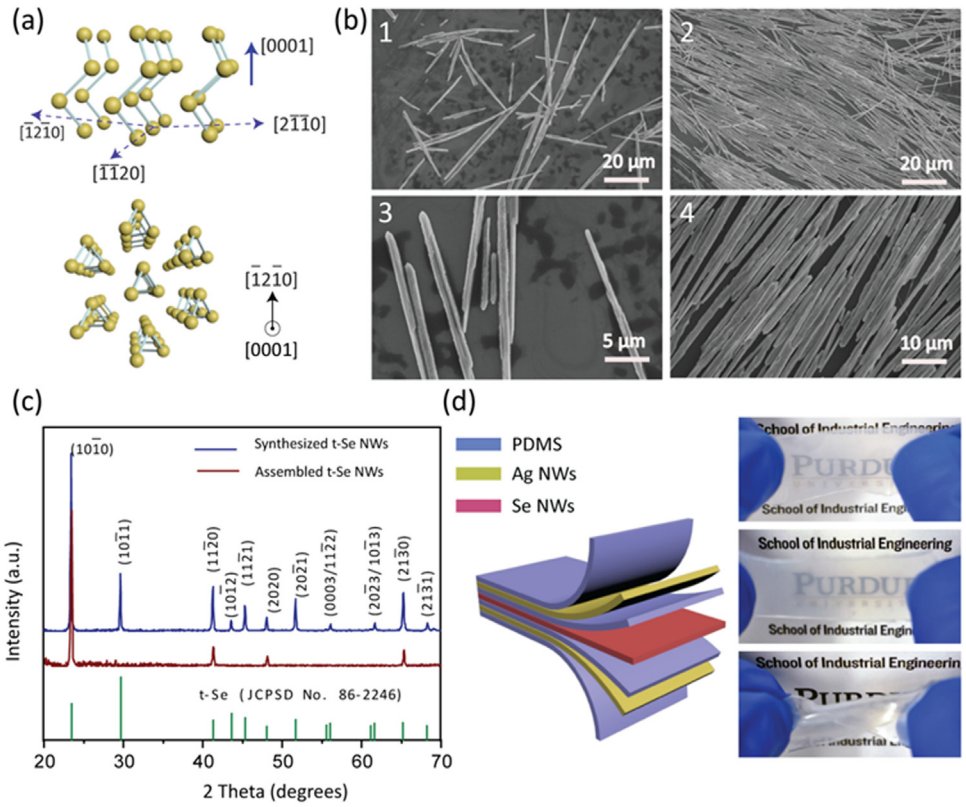

Fig. 1. (a) Schematic of the crystal structure of Se nanowires. (b) SEM images of the as-synthesized Se nanowires and the assembled Se nanowires film. (c) XRD patterns of the as-synthesized Se nanowires and assembled film. (d) 3D illustration of the Se-PENG device and the optical images of the device at the original state, being stretched and twisted, respectively.

applications, e.g., physiological monitoring. The ultrathin device can be conformably worn onto the human wrist, effectively converting the imperceptible time-variant mechanical vibration from the human body into distinguishable electrical signals through straining the piezoelectric Se nanowires.

The trigonal-structured selenium (t-Se) has an anisotropic crystal lattice where individual chiral chains of Se atoms are stacked together by weak bonding [27,28] (Fig. 1a). Each Se atom is covalently bonded with its two nearest neighbors on the same chain. t-Se has the same non-centrosymmetric structure to that of trigonal-structured tellurium (t-Te) [29,30]. Lee et al. previously demonstrated the application of t-Te nanowires for piezoelectric nanogenerator [31]. The solution-synthesized t-Te nanowires are assembled horizontally on the flexible polyimide substrates, and can generate a power density up to 9 mW/cm^3 upon straining. However, the narrow bandgap [32] of metalloid tellurium may limit the piezoelectric application of t-Te nanowires. In contrast, selenium has a sizeable bandgap of 1.7 eV [33,34], and the nanostructured t-Se is expected to exhibit strong piezoelectric property [35], leading to a potential high volume-power-density in integrated devices. Similar to the t-Te nanowire, the radial distribution of the piezoelectric polarization in the t-Se nanowire, due to the strain-induced relative displacement of the electron distribution against the Se atoms cores [36], facilitates its integration into ultrathin laminated devices through economic manufacturing approaches, e.g., roll-to-roll (R2R) printing, onto various substrates [37].

2. Results and discussion

The Se nanowires were synthesized following the procedures described in the Methods section. The morphology of the as-synthesized Se nanowires can be seen in Fig. 1b. The length of the nanowires ranges from tens of μm to 100 μm, while the diameter is ~ 500 nm. Fig. 1 b-1 and b-3 present the morphology of the Se nanowires before the assembly, and Fig. 1 b-2 and b-4 show the Se nanowires after the LB assembly forming a close-packed film with oriented Se nanowires. X-Ray diffraction (XRD) was used to characterize the structure of the product. All the peaks in the XRD pattern (blue line) in Fig. 1c can be assigned to the pure trigonal phase of Se with lattice parameters of a = 4.36 Å and c = 4.97 Å (JCPDS 86-2246). No XRD peaks arising from impurities could be detected, indicating that only elemental Se nanowires with high crystallinity and purity were derived. Compared with the standard pattern of t-Se, it is found that the intensity of (hki0) reflection peaks of our synthesized Se nanowires is strong, which suggests that the as-obtained t-Se crystals have a preferential growth orientation of [0001]. Interestingly, when the Se nanowires are assembled and transferred onto the substrate, some high-index peaks vanish in the XRD pattern (red line in Fig. 1c) with the two most prominent peaks arising from the ($10\bar{1}0$) and ($11\bar{2}0$) planes. Such changes in the XRD patterns are consistent with the observed alignment of the Se nanowires in the horizontal plane after the LB assembly (Fig. 1b).

The piezoelectricity origin can be analyzed from the crystal structure and point group of the material that belongs to. Trigonal selenium belongs to point group of 32, and the space group is either $P3_121$ or $P3_221$. The single crystal material belonging to group 32 has two independent piezoelectric components, d_{11} and d_{14}. The crystal structure of the selenium is demonstrated in Fig. 1a. Two adjacent Se atoms in one spiral are nearest neighbors and stronger bound than adjacent Se atoms of two neighboring spirals (Upper part in Fig. 1a). The hexagonal cross-section of the t-Se NW and its two-dimensional hexagonal-lattice structure with equilateral triangles resulting from the projection of the helical turns of Se atoms onto (0001) planes are illustrated in the lower part of Fig. 1a. We draw a schematic here showing how the selenium atoms in one chain are distorted when they are subject to external stress (Fig. 2a). We use a right-hand coordinate system x, y, z in which x and z correspond to the crystallographic a- and c-axes, respectively. When longitudinal stress is applied along the x-axis, internal displacement of the Se atom and displacement of the electronic charge against the Se cores will occur, which would give rise to a piezoelectric polarization parallel to x-axis. This polarization is described by the piezoelectric coefficient d_{11}. As presented in Fig. 2a(ii) and 2a(iii), when the

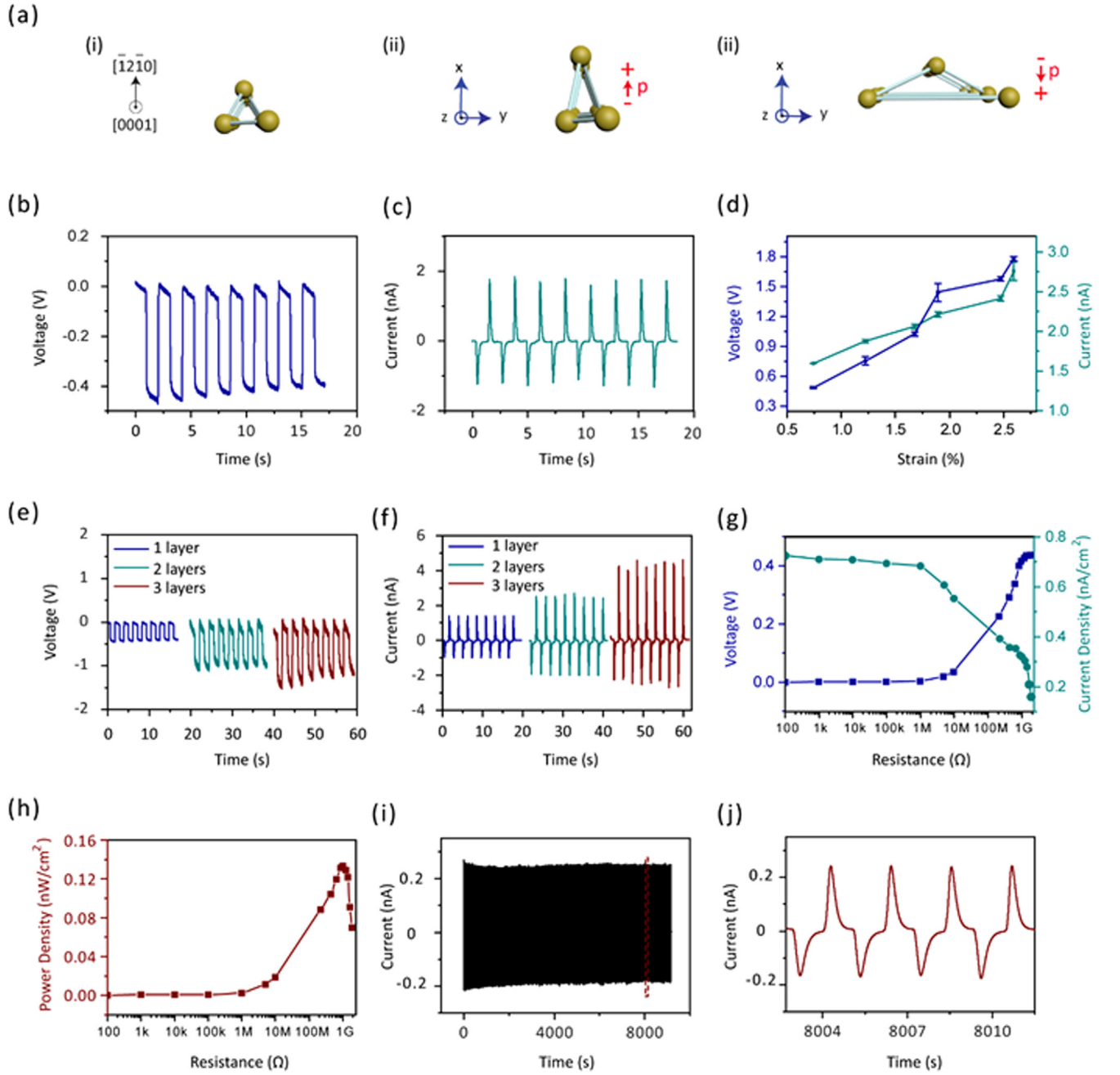

Fig. 2. (a) Schematic showing the deformed Se nanowire chain and the origin of the piezoelectric polarization. (b) open-circuit voltage (V_{oc}) and (c) short-circuit current (I_{sc}) of Se-PENGs. (d) The V_{oc} and I_{sc} as a function of strain. The output (e) voltage and (f) current are from devices with 1, 2 and 3 layers of assembled Se nanowires. (g) The output voltage/current and (h) power versus the load resistance. (i) The cyclic output of Se-PEND during a stability test. (j) The magnified view of the output signals highlighted in (i). Only one layer of Se nanowires is adopted in the device in g, h and i, and the applied mechanical strain is 0.75% for the measurement.

selenium nanowire is stretched vertically, a piezoelectric polarization pointing upward would be generated, and similarly a vertically compressed selenium nanowire would give rise to a downward-pointed piezoelectric polarization. As reported elsewhere, the piezoelectric components, d_{11} is found to be $(0.41 \pm 0.03) \times 10^{(-10)}$ m/V [38]. Although the piezoelectricity of selenium bulk crystal has already been reported in the prior work [35,38–40], this is our first time to report the piezoelectricity in selenium nanowire and fabricate wearable devices for energy harvesting and sensor applications.

The detailed process for fabricating the wearable PENG device based on Se nanowires (Se-PENG) is shown in the experimental section. Our Se-PENG device (Fig. 1d) consists of multiple layers stacking of PDMS, Ag nanowires electrodes, and piezoelectric Se nanowires, which are highly flexible and stretchable. Fig. 1d shows the good deformability of our Se-PENG device which can withstand large degrees of mechanical deformation without fracture or cleavage. A cross-sectional SEM image of the layered device is demonstrated in Fig. S1, and we find that the interface of Se nanowires/PDMS and Ag nanowires/PDMS are visible. To better quantitatively characterize the mechanical properties of the fabricated device, a tensile test is applied here (Fig. S2), where the tensile strength and the maximum strain of the device that can withstand are nearly 1.78 MPa and 200%, respectively. Here the PDMS layers not only serve as the insulating layers between the Se and Ag nanowires but also encapsulate the Ag nanowires from oxidation and

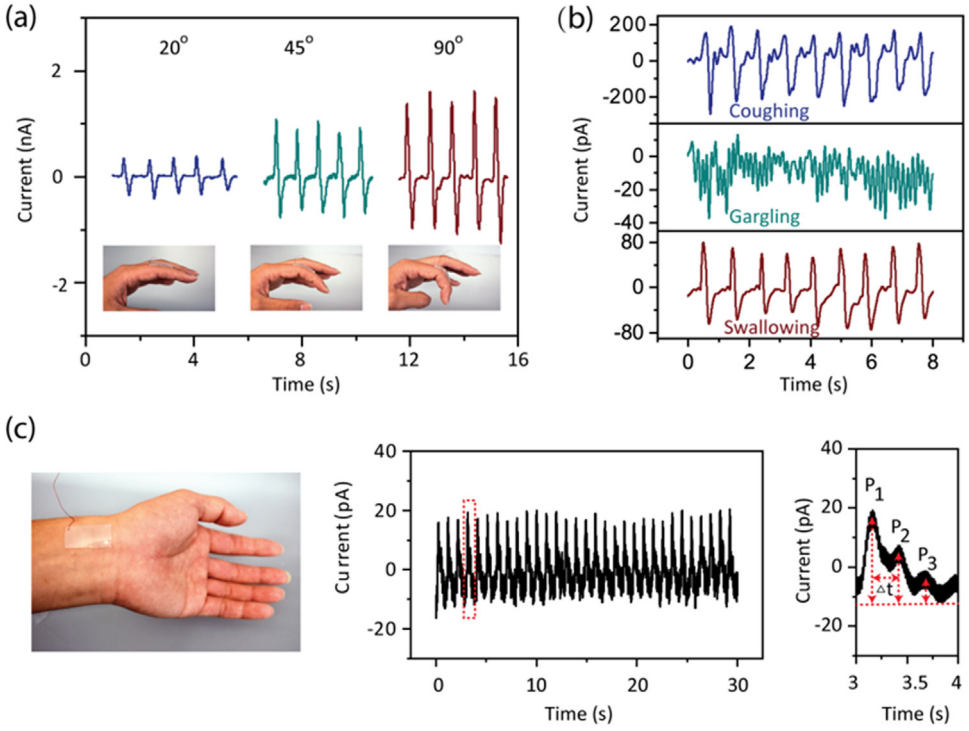

Fig. 3. (a) The output current of the Se-PENG attached on the human fingers and bent with different angles. (b) The output current of the Se-PENG attached on the human throat when the subject is coughing, gargling and swallowing. (c) The real-time artery pulse signal monitored by the Se-PENG.

performance deterioration. In our device, the sprayed Ag nanowires form an interconnected conducting network (Fig. S3, Supporting Information). The entanglement of these long Ag nanowires (lengths ~ 50–100 μm) is expected to lead to a good conductivity and stretchability in the electrodes structure desirable for the PENG application [41]. We also characterized the reliability of our stretchable Ag nanowires electrodes by measuring their resistance after cyclic straining (Fig. S4). A slight increase in electrode resistance was observed after the device being subjected to cyclic large-degree straining, and no observable increase in the electrode resistance can be seen after an initial "burn-in" period of 150-cycle straining. The increase in the Ag nanowire electrode resistance is negligible compared to the internal impedance of the PENG devices (from several hundred MΩ to GΩ) [42–44] and is expected to not affect the output of Se-PENG devices.

Devices with a dimension of 1 cm × 2 cm were used in our experiment for characterizing the piezoelectric output of Se-PENGs. When the devices are subjected to periodic strains with controlled magnitudes, which are applied through a linear motor (Methods), the strain-induced piezoelectric polarizations in the Se nanowires will electrostatically induce an electrical field between the top and bottom electrodes. Such a time-variant piezoelectric field due to the periodic strain leads to the displacement current in the circuit and hence the measured electrical outputs [19]. With a compressive strain of 0.74% along the alignment direction of Se nanowires, the measured open-circuit voltage (V_{oc}) and short-circuit current (I_{sc}) present to be 0.45 V and 1.67 nA, respectively (Fig. 2b and c). The switching-polarity test was further performed to verify that the measured electrical outputs are caused by the intrinsic piezoelectric properties of the assembled Se nanowires [45] (Fig. S5, Supporting information). Additional sets of characterizations were also carried out when the Se-PENGs were subjected to a tensile strain along the alignment direction of Se nanowires (Fig. S5, Supporting information), showing that the electric outputs were reversed when the strain was switched from compressive to tensile. The strain-dependent piezoelectric outputs were also characterized for the Se-PENG devices when the strain increased from 0.74% to 2.59% (Fig. 2d). Both the V_{oc} and I_{sc} increase with the strain. The monotonic dependence of the piezoelectric outputs with the magnitudes of the applied strains suggest that the Se-PENG has a good strain resolution and can function as a self-powered mechanical sensor [46]. The small variance seen for each data point in Fig. 2d is likely due to the variations in the electrode resistance (Fig. S4). The unique crystal structure of Se nanowires and the corresponding radial distribution of the piezoelectric field in strained Se nanowires facilitates the integration of multiple Se-PENGs into ultrathin laminated devices with enhanced outputs. Fig. 2e and f show that both the output voltage and current increase when the assembled Se layers scale up. Here the number of selenium nanowire layers can be controlled by the assembly and the following transfer times to the substrate. The output power of Se-PENG delivered to external loads is characterized by varying the load resistance connected in the circuit. Fig. 2g showed the resistance-dependent output voltage and current when the load resistor was swept from 100 Ω to 1.88 GΩ. The instantaneous output power can then be calculated and plotted as a function of the load resistance (Fig. 2h), with a maximum output power determined to be 0.135 nW/cm^2 at a load resistance of 1 GΩ. Taking advantage of the superior mechanical deformability and stability of the Se nanowire active layer, the Ag nanowires electrodes, and the PDMS layer, Se-PENG shows good long-term stability after being subjected to cyclic straining and release for more than two hours (Fig. 2i and j). No observable damage or deterioration is observed in the morphology of the Se NW encapsulated in the PDMS after repeated large deformation and recovery of the device (Fig. S6). At this moment, the piezoelectric device based on assembled t-Se nanowire layer can stably generate a voltage output equal to 0.45 V, which are already comparable to the output of a couple of previously reported 1D/2D materials (Table S1). Considering the stable voltage output and the unique radial distribution of piezoelectric polarization, we believe that the t-Se nanowire may open doors for the new piezoelectric and piezotronic devices design and integration.

Finally, we explore the feasibility of Se-PENG device for potential self-powered human-integrated applications, e.g., gesture recognition and cardiovascular monitoring. The wearable Se-PENG device can be attached to different parts of human body compliable with minimum

deformation. Fig. 3a shows the application of the Se-PENG device attached to the joint of a finger for detecting and recognizing the finger movement [47]. During the test, the finger was bent to different degrees, and the corresponding outputs were recorded. A larger bending angle gives rise to a stronger piezoelectric output (Fig. 3a). The Se-PENG device can also be attached to the throat for identifying different vocal activities, e.g., coughing, gargling, and swallowing (Fig. 3b). Furthermore, the Se-PENG device can be used to sense the radial artery pulses in real-time (Fig. 3c). The device was attached to the wrist of a healthy 24-year-old male for the non-invasive detection of pulse without using an external power source. The real-time piezoelectric current output from the device for 30 s shows the reliable detection and measurement of the human pulse signals, with distinct three-peak characteristics for the cardiac cycle (Fig. 3c). Such a pattern is consistent with the reported results [48,49] and manifests important information for the health diagnostics. Here we attempted to analyze the acquired signals. Three distinguishable determinants could be obtained from one typical pulse cycle [50–52]: namely, early systolic peak pressure ($P_1(t_1)$: percussion wave (P-wave)), late systolic augmentation shoulder ($P_2(t_2)$: tidal wave (T-wave)), and diastolic pulse waveform ($P_3(t_3)$: diastolic wave (D-wave)). These peaks can be used to quantify the augmentation index ($AI_r = P_2/P_1$) and the time delay between the first and second peaks ($\triangle t = t_2 - t_1$), which provide valuable information for evaluating the physiological conditions of the human cardiovascular system [52–54]. The calculated AI_r and $\triangle t$ using Se-PENG are 0.57 and 0.26 s, respectively, which fall in a normal and healthy range [52–54]. The demonstrated self-powered sensing capability to detect the small-scale biomechanical signals from the human body, together with the facile and low-cost fabrication process, can potentially lead to broader applications of our devices for wearable self-powered biomedical devices.

3. Conclusion

In summary, Se nanowires synthesized by a hydrothermal method are explored as a new class of piezoelectric nanomaterial. The assembled Se nanowires by an LB approach are integrated into a wearable piezoelectric device for PENG application and sensing the small-scale biomechanical signals from the human body. A monolayer of assembled Se film can generate a V_{oc} and I_{sc} up to 0.45 V and 1.7 nA, respectively, when being subjected to a strain of 0.75%, with the maximum power density ~ 0.135 nW/cm^2. The performance and efficiency of such Se-PENG can be optimized by scaling up the number of the active Se layer through the integration of laminated devices. The Se-PENG demonstrated here shows great potential for self-powered biomedical devices, and opens doors to new technologies in energy, electronics, and sensor applications.

4. Methods

4.1. Synthesis of Se nanowires

The synthesis of Se nanowire follows procedures similar to previous report [55] with modified synthesis parameters to achieve a uniform dimension of the as-synthesized nanowires. Specifically, selenium dioxide (SeO_2), glucose ($C_6H_{12}O_6$), and poly(vinylpyrrolidone) (PVP, MW ≈ 55 000) were dissolved in a mixture of deionized (DI) water and ethanol. After constant stirring for 20 mins, 5 mL ammonia ($NH_3{\cdot}H_2O$, 69%) was added into the solution to adjust the pH value. The mixture solution was then transferred to a Teflon-lined autoclave and heated to 160 °C for 20 h. After the reaction, the product was collected by centrifugation and washed several times with DI water to remove the impurities. All the chemicals were purchased from Sigma-Aldrich and used as received.

4.2. Assembly of Se nanowires

After obtaining the centrifuged Se nanowires products, N, N-dimethylformamide (DMF) was added to disperse the Se nanowires and form a homogeneous solution. Chloroform ($CHCl_3$) was then added into the homogeneous solution, which was ready for the subsequent Langmuir-Blodgett (LB) assembly and transfer of Se nanowires onto the various substrates for further characterization.

4.3. Materials characterizations

Morphology and structural characterization of the as-synthesized Se nanowires was performed using a field emission scanning electron microscope (Hitachi S-4800) and a wide-angle X-ray diffractometer in the 20–70° range (Bruker, D8 Advance Diffractometer).

4.4. Fabrication and electric measurement of Se-PENG

Firstly, a thin layer of PDMS was spin-coated onto a PET substrate. After curing at 90 °C, the PDMS layer was treated with oxygen plasma for deriving a hydrophilic surface. Afterward, a layer of Ag nanowires network was spray-coated to function as the bottom electrode. Then, another layer of PDMS was deposited onto the Ag nanowire layer and cured. Subsequently, the Se nanowires layer was transferred onto the polymer stack through the above LB method. The second layer of PDMS was spin-coated onto the Se nanowires layer, then cured and treated with oxygen plasma before the deposition of the top Ag nanowires electrode. To complete the device fabrication, the uppermost PDMS layer was prepared with the same spin-coating method to encapsulate the whole device. The electrical outputs of the Se-PENG were measured using an electrometer (Keithley 6514) and a low-noise current preamplifier (Stanford Research Systems, SR570). A linear motor (LinMot) was used for applying strain to the device.

Acknowledgments

W. Z. W. acknowledges the College of Engineering and School of Industrial Engineering at Purdue University for the startup support. W. Z. W. was partially supported by the National Science Foundation under grant CMMI- 1762698.

Appendix A. Supporting information

Supplementary data associated with this article can be found in the online version at doi:10.1016/j.nanoen.2018.12.003.

References

[1] Z.L. Wang, J. Song, Piezoelectric nanogenerators based on zinc oxide nanowire arrays, Science 312 (5771) (2006) 242–246.
[2] C.-T. Huang, J. Song, W.-F. Lee, Y. Ding, Z. Gao, Y. Hao, L.-J. Chen, Z.L. Wang, GaN nanowire arrays for high-output nanogenerators, J. Am. Chem. Soc. 132 (13) (2010) 4766–4771.
[3] L. Lin, C.-H. Lai, Y. Hu, Y. Zhang, X. Wang, C. Xu, R.L. Snyder, L.-J. Chen, Z.L. Wang, High output nanogenerator based on assembly of GaN nanowires, Nanotechnology 22 (47) (2011) 475401.
[4] M. Minary-Jolandan, R.A. Bernal, I. Kuljanishvili, V. Parpoil, H.D. Espinosa, Individual GaN nanowires exhibit strong piezoelectricity in 3D, Nano Lett. 12 (2) (2012) 970–976.
[5] Y.-F. Lin, J. Song, Y. Ding, S.-Y. Lu, Z.L. Wang, Piezoelectric nanogenerator using CdS nanowires, Appl. Phys. Lett. 92 (2) (2008) 022105.
[6] Y.F. Lin, J. Song, Y. Ding, S.Y. Lu, Z.L. Wang, Alternating the output of a CdS nanowire nanogenerator by a white-light-stimulated optoelectronic effect, Adv. Mater. 20 (16) (2008) 3127–3130.
[7] K.-I. Park, S. Xu, Y. Liu, G.-T. Hwang, S.-J.L. Kang, Z.L. Wang, K.J. Lee, Piezoelectric BaTiO3 thin film nanogenerator on plastic substrates, Nano Lett. 10 (12) (2010) 4939–4943.
[8] S.-H. Shin, Y.-H. Kim, M.H. Lee, J.-Y. Jung, J. Nah, Hemispherically aggregated BaTiO3 nanoparticle composite thin film for high-performance flexible piezoelectric nanogenerator, ACS nano 8 (3) (2014) 2766–2773.
[9] G. Zhang, Q. Liao, Z. Zhang, Q. Liang, Y. Zhao, X. Zheng, Y. Zhang, Novel

piezoelectric paper-based flexible nanogenerators composed of BaTiO3 nanoparticles and bacterial cellulose, Adv. Sci. 3 (2) (2016) 1500257.
[10] M. Zhang, T. Gao, J. Wang, J. Liao, Y. Qiu, H. Xue, Z. Shi, Z. Xiong, L. Chen, Single BaTiO3 nanowires-polymer fiber based nanogenerator, Nano Energy 11 (2015) 510–517.
[11] J.M. Wu, C. Xu, Y. Zhang, Z.L. Wang, Lead-free nanogenerator made from single ZnSnO3 microbelt, ACS Nano 6 (5) (2012) 4335–4340.
[12] M.M. Alam, S.K. Ghosh, A. Sultana, D. Mandal, Lead-free ZnSnO3/MWCNTs-based self-poled flexible hybrid nanogenerator for piezoelectric power generation, Nanotechnology 26 (16) (2015) 165403.
[13] K.Y. Lee, D. Kim, J.H. Lee, T.Y. Kim, M.K. Gupta, S.W. Kim, Unidirectional high--power generation via stress-induced dipole alignment from ZnSnO3 nanocubes/polymer hybrid piezoelectric nanogenerator, Adv. Funct. Mater. 24 (1) (2014) 37–43.
[14] M. Wu, T. Zheng, H. Zheng, J. Li, W. Wang, M. Zhu, F. Li, G. Yue, Y. Gu, J. Wu, High-performance piezoelectric-energy-harvester and self-powered mechanosensing using lead-free potassium–sodium niobate flexible piezoelectric composites, J. Mater. Chem. A 6 (34) (2018) 16439–16449.
[15] Y. Huan, X. Zhang, J. Song, Y. Zhao, T. Wei, G. Zhang, X. Wang, High-performance piezoelectric composite nanogenerator based on Ag/(K,Na)NbO3 heterostructure, Nano Energy 50 (2018) 62–69.
[16] C. Chang, V.H. Tran, J. Wang, Y.-K. Fuh, L. Lin, Direct-write piezoelectric polymeric nanogenerator with high energy conversion efficiency, Nano Lett. 10 (2) (2010) 726–731.
[17] S. Cha, S.M. Kim, H. Kim, J. Ku, J.I. Sohn, Y.J. Park, B.G. Song, M.H. Jung, E.K. Lee, B.L. Choi, J.J. Park, Z.L. Wang, J.M. Kim, K. Kim, Porous PVDF As effective sonic wave driven nanogenerators, Nano Lett. 11 (12) (2011) 5142–5147.
[18] M. Lee, C.Y. Chen, S. Wang, S.N. Cha, Y.J. Park, J.M. Kim, L.J. Chou, Z.L. Wang, A hybrid piezoelectric structure for wearable nanogenerators, Adv. Mater. 24 (13) (2012) 1759–1764.
[19] Z.L. Wang, On Maxwell's displacement current for energy and sensors: the origin of nanogenerators, Mater. Today 20 (2) (2017) 74–82.
[20] Y. Qi, N.T. Jafferis, K. Lyons Jr, C.M. Lee, H. Ahmad, M.C. McAlpine, Piezoelectric ribbons printed onto rubber for flexible energy conversion, Nano Lett. 10 (2) (2010) 524–528.
[21] Y. Hu, Y. Zhang, C. Xu, G. Zhu, Z.L. Wang, High-output nanogenerator by rational unipolar assembly of conical nanowires and its application for driving a small liquid crystal display, Nano Lett. 10 (12) (2010) 5025–5031.
[22] V. Nguyen, R. Zhu, K. Jenkins, R. Yang, Self-assembly of diphenylalanine peptide with controlled polarization for power generation, Nat. Commun. 7 (2016) 13566.
[23] Y. Hu, Y. Zhang, C. Xu, L. Lin, R.L. Snyder, Z.L. Wang, Self-powered system with wireless data transmission, Nano Lett. 11 (6) (2011) 2572–2577.
[24] X. Wang, Piezoelectric nanogenerators—harvesting ambient mechanical energy at the nanometer scale, Nano Energy 1 (1) (2012) 13–24.
[25] B.J. Hansen, Y. Liu, R. Yang, Z.L. Wang, Hybrid nanogenerator for concurrently harvesting biomechanical and biochemical energy, ACS Nano 4 (7) (2010) 3647–3652.
[26] Y. Hu, Z.L. Wang, Recent progress in piezoelectric nanogenerators as a sustainable power source in self-powered systems and active sensors, Nano Energy 14 (2015) 3–14.
[27] P. Cherin, P. Unger, The crystal structure of trigonal selenium, Inorg. Chem. 6 (8) (1967) 1589–1591.
[28] B.T. Mayers, K. Liu, D. Sunderland, Y. Xia, Sonochemical synthesis of trigonal selenium nanowires, Chem. Mater. 15 (20) (2003) 3852–3858.
[29] Z. Wang, L. Wang, H. Wang, PEG-mediated hydrothermal growth of single-crystal tellurium nanotubes, Cryst. Growth Des. 8 (12) (2008) 4415–4419.
[30] Z. Li, S. Zheng, Y. Zhang, R. Teng, T. Huang, C. Chen, G. Lu, Controlled synthesis of tellurium nanowires and nanotubes via a facile, efficient, and relatively green solution phase method, J. Mater. Chem. A 1 (47) (2013) 15046–15052.
[31] T.I. Lee, S. Lee, E. Lee, S. Sohn, Y. Lee, S. Lee, G. Moon, D. Kim, Y.S. Kim, J.M. Myoung, Z.L. Wang, High-power density piezoelectric energy harvesting using radially strained ultrathin trigonal tellurium nanowire assembly, Adv. Mater. 25 (21) (2013) 2920–2925.
[32] H.G. Junginger, Electronic band structure of tellurium, Solid State Commun. 5 (7) (1967) 509–511.
[33] J.R. Reitz, Electronic band structure of selenium and tellurium, Phys. Rev. 105 (4) (1957) 1233–1240.
[34] S. Kumar, Synthesis and characterisation of selenium nanowires using template synthesis, J. Exp. Nanosci. 4 (4) (2009) 341–346.
[35] D. Royer, E. Dieulesaint, Elastic and piezoelectric constants of trigonal selenium and tellurium crystals, J. Appl. Phys. 50 (6) (1979) 4042–4045.
[36] S. Gao, Y. Wang, R. Wang, W. Wu, Piezotronic effect in 1D van der Waals solid of elemental tellurium nanobelt for smart adaptive electronics, Semicond. Sci. Technol. 32 (10) (2017) 104004.
[37] S. Bae, H. Kim, Y. Lee, X. Xu, J.-S. Park, Y. Zheng, J. Balakrishnan, T. Lei, H.R. Kim, Y.I. Song, Roll-to-roll production of 30-inch graphene films for transparent electrodes, Nat. Nanotechnol. 5 (8) (2010) 574.
[38] J. Bouat, J. Thuillier, Electromechanical resonance in selenium determination of the piezoelectric coefficient d11, Phys. Lett. A 37 (1) (1971) 71–72.
[39] T. Shiosaki, A. Kawabata, T. Tanaka, Piezoelectric properties of Se film deposited on Te crystal, Jpn. J. Appl. Phys. 9 (6) (1970) 631.
[40] V. Kunigelis, D. Royer, E. Dieulesaint, J. Thuillier, Determination of the piezoelectric constant d14 of trigonal selenium crystals, Phys. Lett. A 56 (4) (1976) 331–332.
[41] F. Xu, Y. Zhu, Highly conductive and stretchable silver nanowire conductors, Adv. Mater. 24 (37) (2012) 5117–5122.
[42] S. Niu, Z.L. Wang, Theoretical systems of triboelectric nanogenerators, Nano Energy 14 (2015) 161–192.
[43] X. He, Y. Zi, H. Guo, H. Zheng, Y. Xi, C. Wu, J. Wang, W. Zhang, C. Lu, Z.L. Wang, A highly stretchable fiber-based triboelectric nanogenerator for self-powered wearable electronics, Adv. Funct. Mater. 27 (4) (2017) 1604378.
[44] X. Chen, K. Parida, J. Wang, J. Xiong, M.-F. Lin, J. Shao, P.S. Lee, A stretchable and transparent nanocomposite nanogenerator for self-powered physiological monitoring, ACS Appl. Mater. Interfaces 9 (48) (2017) 42200–42209.
[45] R. Yang, Y. Qin, C. Li, G. Zhu, Z.L. Wang, Converting biomechanical energy into electricity by a muscle-movement-driven nanogenerator, Nano Lett. 9 (3) (2009) 1201–1205.
[46] Z.L. Wang, W. Wu, Nanotechnology-enabled energy harvesting for self-powered micro-/nanosystems, Angew. Chem. Int. Ed. 51 (47) (2012) 11700–11721.
[47] K.C. Pradel, W. Wu, Y. Ding, Z.L. Wang, Solution-derived ZnO homojunction nanowire films on wearable substrates for energy conversion and self-powered gesture recognition, Nano Lett. 14 (12) (2014) 6897–6905.
[48] G. Schwartz, B.C.-K. Tee, J. Mei, A.L. Appleton, D.H. Kim, H. Wang, Z. Bao, Flexible polymer transistors with high pressure sensitivity for application in electronic skin and health monitoring, Nat. Commun. 4 (2013) 1859.
[49] J. Park, M. Kim, Y. Lee, H.S. Lee, H. Ko, Fingertip skin–inspired microstructured ferroelectric skins discriminate static/dynamic pressure and temperature stimuli, Sci. Adv. 1 (9) (2015) e1500661.
[50] G.M. London, A.P. Guerin, Influence of arterial pulse and reflected waves on blood pressure and cardiac function, Am. Heart J. 138 (3) (1999) S220–S224.
[51] A.P. Avolio, M. Butlin, A. Walsh, Arterial blood pressure measurement and pulse wave analysis—their role in enhancing cardiovascular assessment, Physiol. Meas. 31 (1) (2009) R1.
[52] W.W. Nichols, Clinical measurement of arterial stiffness obtained from noninvasive pressure waveforms, Am. J. Hypertens. 18 (S1) (2005) 3S–10S.
[53] Z. Lin, J. Chen, X. Li, Z. Zhou, K. Meng, W. Wei, J. Yang, Z.L. Wang, Triboelectric nanogenerator enabled body sensor network for self-powered human heart-rate monitoring, ACS Nano 11 (9) (2017) 8830–8837.
[54] P.S. Saba, M.J. Roman, R. Pini, M. Spitzer, A. Ganau, R.B. Devereux, Relation of arterial pressure waveform to left ventricular and carotid anatomy in normotensive subjects, J. Am. Coll. Cardiol. 22 (7) (1993) 1873–1880.
[55] Q. Xie, Z. Dai, W. Huang, W. Zhang, D. Ma, X. Hu, Y. Qian, Large-scale Synthesis and growth mechanism of single-crystal Se nanobelts, Cryst. Growth Des. 6 (6) (2006) 1514–1517.

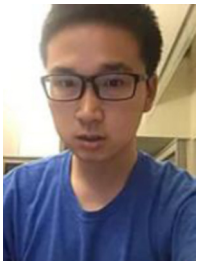

Min Wu received his BS degree in Materials Science and Engineering from the University of Science and Technology Beijing in 2014 and his MS degree in Mechanical and Energy Engineering from the University of North Texas in 2016. He is pursuing his Ph.D. in the School of Industrial Engineering at Purdue University under the supervision of Prof. Wenzhuo Wu. His research interest includes the synthesis of low-dimensional materials and investigation of their piezoelectric properties, nanodevice fabrication and flexible electronics.

Yixiu Wang received his MS degree in Materials Science and Engineering from the University of Science and Technology of China (USTC) under the supervision of Prof. Shu-Hong Yu in 2014. He is currently pursuing his Ph.D. in the School of Industrial Engineering under the supervision of Prof. Wenzhuo Wu. His primary research activity focuses on the low-dimensional material synthesis and novel 2D atomic crystals targeting nanoelectronics and energy conversion devices together with the exploration of fundamental phenomena in nanoscale systems.

Shengjie Gao received his BS degree in Materials Chemistry from Lanzhou University in 2016. He is currently pursuing his Ph.D. in School of Industrial Engineering at Purdue University under the supervision of Prof. Wenzhuo Wu. His research interests include the piezotronics, self-powered system, and human-machine interface.

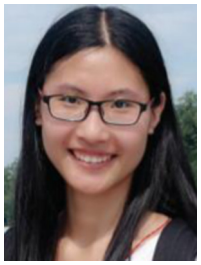

Ruoxing Wang received her BS degree in Chemistry in 2011 from the University of Science and Technology of China (USTC). She is currently a Ph.D. student in Industrial Engineering at Purdue University under the supervision of Prof. Wenzhuo Wu. Her research interests mainly focus on nanomanufacturing including the design of functional nanomaterials and fabrication of nanodevices for various applications.

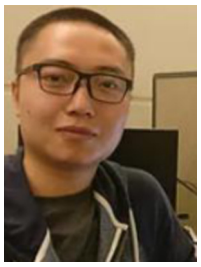

Chengxiang Ma received his BS degree in Chemical Engineering in 2013 from Tianjin University. He is currently pursuing his Ph.D. in School of Chemical Engineering and Technology at Tianjin University. He was a visiting student in Industrial Engineering at Purdue University from 2016 to 2018 under the supervision of Prof. Wenzhuo Wu. His research interests focus on the synthesis of nanomaterials for energy storage devices, and self-powered system.

Dr. Zhiyuan Tang is a professor in School of Chemical Engineering and Technology at Tianjin University. Dr. Tang received his BS degree in 1969 and his MS degree in 1981 in Chemical Engineering from Tianjin University. Dr. Tang's research interests include the materials design and preparation for lithium-ion batteries and safety issue control in the manufacturing process.

Dr. Ning Bao is a professor in the School of Public Health at Nantong University. Dr. Bao received his Ph.D. from Nanjing University in 2005. He did postdoctoral research at Purdue University from 2006 to 2010. Dr. Bao's research interests include microfluidic analysis systems, analytical instrument.

Dr. Wenxuan Wu received his BS degree in 2004 and his Ph.D. in 2011 in Polymer Chemistry and Physics from University of Science and Technology of China. He has been engaged in the R&D work of polymer dispersed liquid crystals (PDLC) materials in the technology companies since 2011. He is currently the deputy general manager of Shenzhen Broadthink Advanced Materials Tech. Co., Ltd. His main research interests focus on PDLC materials, self-assembling materials, chiral materials, and economic production process of the optical films.

Dr. Fengru Fan received his BS degree in 2006 and his Ph.D. in 2013 in Chemistry from Xiamen University. From 2008–2012, he was a visiting student at the Georgia Institute of Technology under the supervision of Prof. Zhong Lin Wang. He is currently a postdoctoral researcher in University of California, Santa Barbara. His main research interests focus on the fields of nanogenerator, nanocrystal, self-powered micro/nano-systems, and nanomaterials in chemistry.

Dr. Wenzhuo Wu is the Ravi and Eleanor Talwar Rising Star Assistant Professor in School of Industrial Engineering at Purdue University. He received his BS in Electronic Information Science and Technology in 2005 from the University of Science and Technology of China (USTC), Hefei and his ME in Electrical and Computer Engineering from the National University of Singapore (NUS) in 2008. Dr. Wu received his Ph.D. from Georgia Institute of Technology in Materials Science and Engineering in 2013. Dr. Wu's research interests include design, manufacturing, and integration of 1D and 2D nanomaterials for applications in energy, electronics, optoelectronics, and wearable devices.